ACEEE Int. J. on Signal & Image Processing, Vol. 4, No. 2, May 2013

Left Ventricle Volume Measurement on Short Axis MRI Images Using a Combined Region Growing and Superellipse Fitting Method

Mostafa Ghelich Oghli[1, 2], Alireza Fallahi[3], Vahab Dehlaghi[2] , and Mohammad Pooyan[4]
[1] Students Research Committee, Kermanshah University of Medical Sciences, Kermanshah, Iran
[2] Kermanshah University of Medical Sciences, Kermanshah, Iran
Email: m.g31_mesu@yahoo.com
Email: dr.dehlaqi@yahoo.com
[3] Department of Biomedical Engineering, Hamedan University of Technology, Hamedan, Iran
Email: ali.r.fallahi@gmail.com
[4] Department of Biomedical Engineering, Shahed University, Tehran, Iran
Email: pooyan@shahed.ac.ir

Abstract— **Segmentation and volume measurement of the cardiac ventricles is an important issue in cardiac disease diagnosis and function assessment. Cardiac Magnetic Resonance Imaging (CMRI) is the current reference standard for the assessment of both left and right ventricular volumes and mass. Several methods have been proposed for segmentation and measurement of cardiac volumes like deformable models, active appearance, shape models, atlas based methods, etc. In this paper a novel method is proposed based on a parametric superellipse model fitting for segmentation and measurement volume of the left ventricle on cardiac Cine MRI images. Superellipses can be used to represent in a large variety of shapes. For fitting superellipse on MR images, a set of data points have been needed as a partial data. This data points resulted from a semi-automatic region growing method that segment the homogenous region of the left ventricle. Because of ellipsoid shape of left ventricle, fitting superellipse on cardiac cine MRI images has excellent accuracy. The results show better fitting and also less computation and time consuming compared to active contour methods, which is commonly used method for left ventricle segmentation.**

Index Terms— **Cardiac MRI, Volume measurement, Deformable superellipse, Levenberg Marquardt algorithm, Region Growing, Gray space map**

I. Introduction

Cardiovascular disease is a major cause of death in the western world, which is responsible for nearly half of all deaths in Europe and approximately a third of all deaths in USA. There are several modalities for diagnosing cardiovascular diseases such as magnetic resonance imaging (MRI), computed tomography (CT), angiography and etc. Many radiologists investigate MRI images, searching for representative projection of the heart and its chambers (right and left ventricles and atriums).

The computation of clinical parameters to assess the cardiac function requires segmenting the cardiac ventricles. As the heart is a moving organ, images are acquired throughout the whole cardiac cycle, but two precise instants are of particular interest for the clinician: the time of maximum filling, when the heart is the most dilated (end diastole, ED), and the time of greatest contraction (end systole, ES). To estimate these volumes it is necessary to apply invasive or non-invasive medical investigation techniques. The segmentation of ED and ES images of the Right Ventricles (RV) is currently performed manually in clinical routine. This long and tedious task, prone to intra- and inter-expert variability, requires about 20 min per ventricle by an expert clinician. The great need for automated methods has led to the development of a wide variety of segmentation methods [1]. Most of these methods compute a pixel wise correspondence between the current image (or frame) and model distributions of photometric (intensity based) and geometric properties of the target objects. In this area, methods can be categorized in thresholding [2], pixel classification [3–4], deformable models and atlas based segmentation. Among these methods deformable models have been greatly used as their flexibility, especially for this application [5–7], either on the form of 2D active contours or 3D deformable surfaces. A review of papers on deformable models can be found in [8]. One of the disadvantages of these methods are being computationally expensive [9, 10] and reinitialization problem, that make them time consuming. Nonhomogenity region and missing boundary is other problems that affect result efficiency. Several works have been performed in literature in left ventricle volume measurement area. One of these methods is Active Shape Model (ASM) and Active Appearance Model (AAM). ASM consist of a statistical shape model, called Point Distribution Model (PDM), obtained by a PCA on the set of aligned shapes, and a method for searching the model in an image [11. Segmentation is performed by placing the model on the image, and iteratively estimating parameters using least square estimation. ASM have been extended to gray level modeling, yielding Active appearance models (AAM) [12], that represent both the shape and texture variability seen in a training set. This technique ensures to have a realistic solution, since only shapes similar to the training set are allowed. In [13], the authors introduce a multistage hybrid model, arguing that AAM are optimized on global appearance but provide

DOI: 01.IJSIP.4.2.1219

imprecise border locations, whereas ASM have a great ability to find local structures. They thus propose to concatenate several independent matching phases, starting with an AAM early stage that positions the model onto the heart, followed by a hybrid ASM/AAM stage that allows for position refinement. A final stage of AAM aids in escaping a possible local minimum found during the ASM/AAM stage. Although this method provides accurate results, and, for the first time with AAM, results on the RV, the current model training has been limited to mid-ventricular, end diastolic images. Estimation models have been done by Dulce et al [14]. They compared magnetic resonance data sets by using a modified Simpson-Rule on a biplane ellipsoid model and the 3D data set of MR images. Goshtasby et al. [15] applied a two-stage algorithm for extraction of the ventricular chambers in flow-enhanced MR images. They approximate location and size of endocardialy surfaces by intensity thresholding and reposition points on the approximated surfaces to nearest local gradient maxima. Then they fit a cylinder into the point set. Weng et al. [16] proposed a learning based ventricle detection from MR and CT images based on a likelihood measure for region-of-interest detection. The contributions regarding ventricle segmentation using deformable models have mainly dealt with the design of the data-driven term. Initially gradient based [17] and thus sensitive to noise, region-based terms have been introduced, that is based on a measure of region homogeneity [18]. In [19], the authors take into account the intensity distribution overlap that exists between myocardium and cavity, and background and myocardium, and introduce a new term in the functional that measures how close the overlaps are to a segmentation model, manually obtained in the first frame. A comprehensive review of segmentation methods in short axis cardiac MR images can be found in [20]. In this paper we used a parametric superellipse model, for fitting on left ventricle. Superellipses are a flexible representation that naturally generalizes ellipses. They can model a large variety of natural shapes, including ellipse, rectangles, parallelograms, and pinched diamonds, by changing a small number of parameters [21]. Hence, the superellipse is a flexible primitive in machine vision and image processing. In addition, the squareness of the superellipse is similar to the eccentricity of an ellipse, which is very useful for pattern recognition. Superellipses were first formulated by Gardiner [22]. The three-dimensional superellipsoid version was popularized in computer graphics by Barr [23] and in computer vision by Pentland [24]. Several approaches have been suggested to determine the parameters of superellipses. In its original form, a superellipse is fitted using the least mean square (LMS) method, and the parameters are determined by minimizing the errors between the curve and the real data. Orthogonal and algebraic distances are used to calculate the errors [25]. When only partial data (data points) is available the parameter estimation and Fitting superellipse to the data become unreliable [26]. There are several methods that can provide partial data for fitting superellipse on them. Some of these methods are manually and need user interaction. But the advanced methods provide data points automatically. In our previous work [27] data points were manually chosen. In this paper we used a semi-automatic region growing method for providing data points that is a well-known method for segmentation of medical and non-medical images [28]. To segment homogenous regions, semi-automatic region growing method is used which requires user interaction to identify initial seed point. After determining the seed pixels, the region growing algorithm applied using gray scale, spatial information and Otsu thresholding method for segmenting the region [29]. After applying morphology operation, border of the segmented region have been used as initial data points for fitting superellipse. In the next step using Levenberg-Marquardt algorithm (LMA) [30] for parameter estimation, superellipse has been fitted on data points. The algorithm diagram can be seen in "Fig. 1,".

II. Initial Segmentation Using Region Growing Method

Basically, region growing operates by merging the nearby pixels that meet a given homogeneity criterion, starting from an initial set of points, known as "seeds". This approach offers several advantages over conventional segmentation techniques. Instead of identifying boundaries, region growing operates always on closed regions in each step of the algorithm, and thus avoids further post-processing to recover the boundaries of disconnected objects. The algorithm is also more stable with respect to noise, and region membership can be based on multiple criteria, facilitating the simultaneous consideration of several features from the image data, and the introduction of eventual a priori knowledge about the structures to be segmented. Our proposed semi automatic region growing algorithm, needs a seed point that identified by operator as shown in "Fig. 2,". Because of almost homogeneous left ventricle region in cine MRI, final result of region growing algorithm is not dependent to the location of seed point and it has minimum effect to the final partial data.

A. Gray Space map

The algorithm of region growing is very simple. We compute the seed gray level: V, then look for structures which have the same gray level than the seed overlapping the seed position. At the second iteration, we look for structures having a small gray level difference from the seed. In other

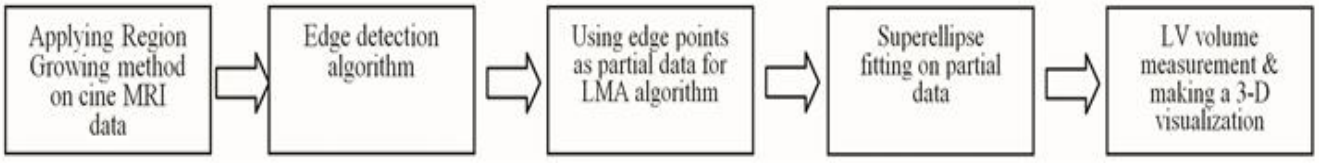

Figure 1. Our proposed method diagram

DOI: 01.IJSIP.4.2.1219

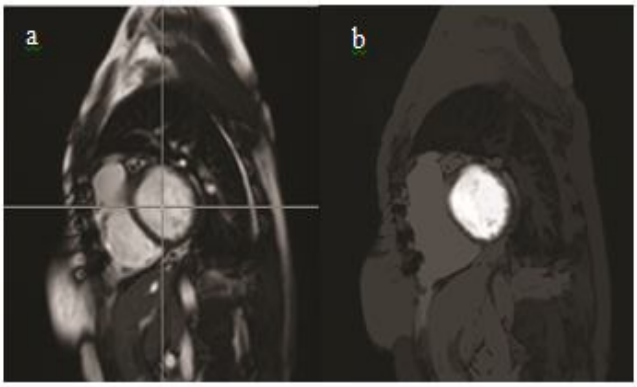

Figure 2. (a) Manually selection of seed point (b) Visualization of Gray Space map

words we define a set of gray levels from "V-D" to "V+D". (D is the difference value). Then we keep those structures which overlap the seed position. In each iterations we increase the difference D by 1. In this way structures which are closed from a spatial AND intensity point of view to the seed are highlighted with higher values [32]. In new image if we far spatially and from an intensity the point of view from the seed, the lower intensity is labeled. Resulted image is Gray Space map of the image, "Fig. 2,". An approach is to verify that even if the labeled area grows, the homogeneity of the area is constant. We try to see statistics of the area during the region growing, when the statistics change too much, it means that we are introducing heterogeneous areas in our region, so we must stop the growing.

In our case we computed the variation of the Euclidean distance between the histograms before and after each growing step [29]. We found this variation to be very similar to the variation of the region area: if we include large areas in our ROI, there is a big area variation, but also, in the same time a big statistic variation. "Fig. 3," shows a classical histogram after the GS map computation. The ROI is highlighted, so it is placed in the higher intensity range.

B. Segmentation

First we find the maximum area variation in "Fig. 3," which means that from this intensity to 0 is not the Region of Interest (ROI). Then we cut the histogram from MAX to intensity 0. We have to find the threshold from MAX to the highest intensity which separates the uncertainty area from the ROI. This is simply done using the well-known Otsu thresholding method. This is a parameter free thresholding technique which maximizes the inter-class variance. Two types of morphological operations are applied to the binary images in order to filling this region. We first applied filling algorithm to fill the holes. The closing algorithm then applied to have a smooth boundary.

C. Border detection

The final step for finding initial data points is determining of segmented region border. This achieved by applying canny edge detection algorithm on segmented region. The results are shown in "Fig. 4".

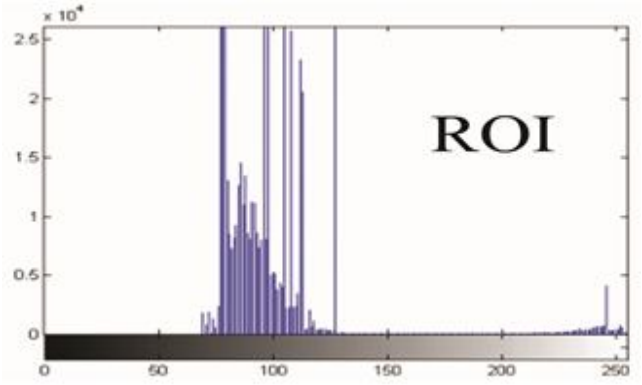

Figure 3. Gray Space(GS) map histogram

III. Superellipse Fitting

Several methods have been proposed for fitting superellipses to the images [31]. We used an iterative Levenberg-Marquardt algorithm [30] (LMA) for parameter estimation. This method provides a numerical solution to the problem of minimizing a function, generally nonlinear, over a space of parameters of the function.

A. Distance criteria

Fitting superellipse on a given set of pixel data using least square solution achieved by finding the set of model parameters that minimize the sum of the squares of the distances between the model curve and given pixel data. The notion of distance can be interpreted in various ways and Rosin and West [33] investigate several examples. The Euclidean distance between a pixel and the point on the superellipse closest to it is probably the most suitable measure. Unfortunately, finding this distance is generally very time consuming and therefore is rarely used. A simpler but still effective measure is the algebraic distance given by

$$\left[\frac{(x-x_c)\cos\theta-(y-y_c)\sin\theta}{a}\right]^{2/\varepsilon}+\left[\frac{(y-y_c)\cos\theta-(x-x_c)\sin\theta}{b}\right]^{2/\varepsilon} \quad (1)$$

Figure 4. Gray Space(GS) map histogram

[33]. Tapering parameter, formulated by equation (2),

$$\begin{cases} x' = \left(ty/a_y + 1\right) x \\ y' = y \end{cases}, \qquad -1 \le t \le 1. \quad (2)$$

DOI: 01.IJSIP.4.2.1219

that minimized by another equation Q_1 by Levenberg Marquardt algorithm. The best fit superellipse is determined by finding the parameters which minimize the objective functional $Q_0(x, y)^2$.

One of the main problems with the algebraic distance is that it results in different distance estimates for different parts of superellipse curves depending on the local curvature of the curve. This is because the conventional algebraic distance measure treats pixels as individual data points and relations between pixels are not exploited. In this paper we propose a modification procedure using adaptive data point selection and parameter λ for more effective convergence of LMA algorithm.

B. Fitting procedure

Like other numeric minimization algorithms, the Levenberg–Marquardt algorithm is an iterative procedure. To start a minimization, initial guess must be provided for the parameter vector, β [30]. In many cases, an uninformed standard guess like β = (1,1,...,1) will work fine; in other cases, the algorithm converges only if the initial guess is already somewhat close to the final solution.

So our fitting procedure consists of 3 steps:

- Determining data points. This step was done by region growing method in pervious section.
- Preparing initial values for Levenberg Marquardt algorithm namely x_c, y_c, a, b, ε, θ, t. Our parameter vector, therefore should be expressed as β{,, a, b, , , t}
- Implementation of Levenberg Marquardt algorithm for finding superellipse parameters.

The initial values are given by user. For our propose an uninformed standard guess like β= (1,1,...,1) will work fine. Also data points are given by user.

After determining data points the Levenberg Marquardt algorithm starts fitting superellipse to partial data. First of all as a problem definition we have a set of data points of independent and dependent variables, (x_i, y_i), optimize the parameters β of the model curve *f*(*x*, β) so that the sum of the squares of the deviations

$$S(\beta) = \sum_{i=1}^{m} \left[y_i - f(x_i, \beta) \right]^2 \qquad (3)$$

becomes minimal.

Levenberg Marquardt algorithm as mentioned is an iterative procedure and needs initial values for parameter vector β. After preparing theses initial values by user algorithm starts its iteration.

In each iteration step, the parameter vector, β, is replaced by a new estimate, β + δ. To determine δ, the functions $f(x_i, \beta + \delta)$ are approximated by their linearization.

$$f(x_i, \beta + \delta) \approx f(x_i, \beta + \delta) + J_i \delta . \qquad (4)$$

Where

$$J_i = \frac{\partial f(x_i, \beta)}{\partial \beta} . \qquad (5)$$

is the gradient (row-vector in this case) of f with respect to β. At a minimum of the sum of squares, called S, the gradient of S with respect to δ is 0. Differentiating the squares in the definition of S, using the above first-order approximation of $f(x_i, \beta + \delta)$, and setting the result leads to:

$$(J^T J)\delta = J^T [y - f(\beta)] . \qquad (6)$$

Where J is the Jacobian matrix whose i-th row equals J_i, and where f and y are vectors with ith component $f(x_i, \beta)$ and y_i, respectively. This is a set of linear equations which can be solved for δ. Levenberg improves the algorithm with replacing this equation by a "damped version",

$$(J^T J + \lambda I)\delta = J^T [y - f(\beta)] . \qquad (7)$$

Where I is the identity matrix, giving as the increment, δ, to the estimated parameter vector, β. The (non-negative) damping factor, λ, is adjusted at each iterations. If reduction of S is rapid, a smaller value can be used, whereas if iteration gives insufficient reduction in the residual, λ can be increased.

"Fig. 5," shows the result of applying our proposed method on a slice of short axis cardiac cine MRI in whole cardiac cycle from end of diastole to end of systole that shows robustness of proposed method for segmentation of left ventricle in different phases of cardiac cycle.

"Fig. 6," shows the result of applying our proposed method on short axis cardiac MRI images of various patients that proves robustness of proposed method for segmentation of left ventricle in different shapes.

IV. Estimating Left Ventricle Volume

The final step is the calculation of the left ventricle volume. Therefore the segmented pixels of all images are counted and multiplied by their voxel size. This segmentation result, define a binary mask on the input images which distinguishes between ventricle and background pixels. In the field of radiology the technique of defining the counting result of voxels to get a volume is called *Simpson Rule*. The DICOM file format stores the voxel size by means of three entries:

- pixel spacing in x- and y-direction (0.83333 mm x 0.83333 mm)
- slice thickness in z-direction (8 mm - 1.2 mm)
- slice gap (0 mm - 4mm)

With this information voxel size is defined as *pixel_spacing_x * pixel_spacing_y * slice_thickness.* The volume generated for this approach can be seen in "Fig. 7,". "Fig. 8," shows result of implementation of region growing algorithm on a not-well-defined left ventricle border short axis cardiac MR image that proves undeniable effect of an

DOI: 01.IJSIP.4.2.1219

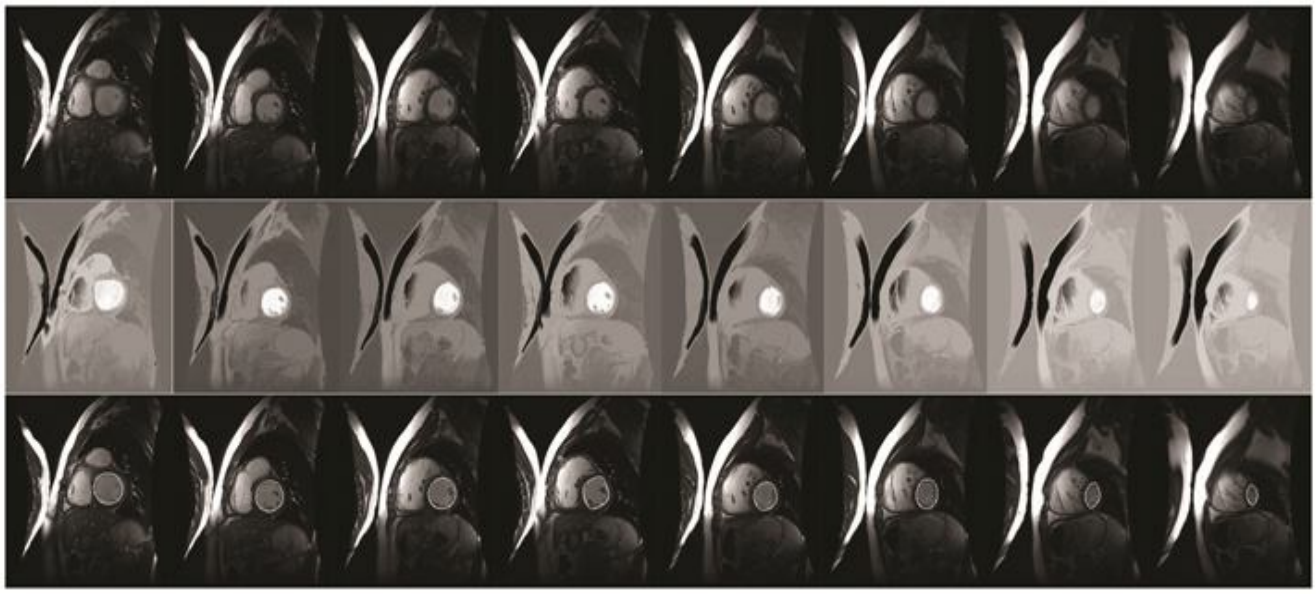

Figure 5. Result of superellipse fitting on left ventricle in whole cardiac cycle: first column: input images, second column: GSmap, third column: final results

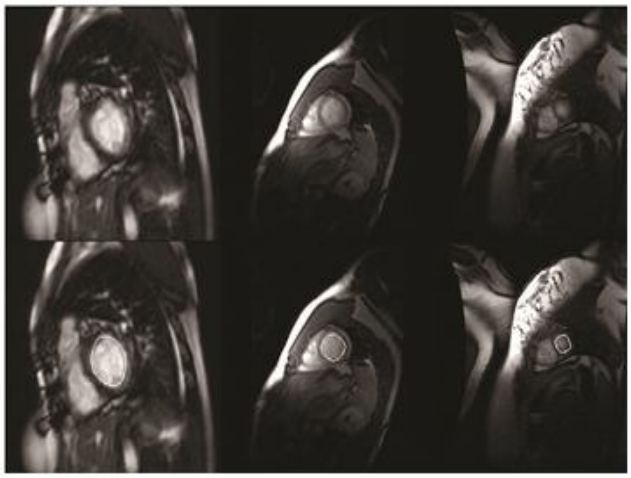

Figure 6. Result of superellipse fitting on left ventricle in various types of cardiac MR images

expert clinician for providing partial data in these cases.

V. Exprimental Results And Discutions

Cardiac cine MRI images are used to evaluate left ventricle volume in this study. Cine MR images provide comprehensible view of a moving organ like heart. The implementation of this method is done using MATLAB 7.12.0. Proposed algorithm is tested on 17 data sets of 17 patients. The images size was 254×254 pixels.

To validate the segmentation results and qualitative comparison, we compared obtained results with manual segmentation performed by a senior radiologist.

Because of ellipsoid shape of left ventricle, fitting superellipse on cardiac cine MRI images has excellent accuracy. Our results show less computation and time consuming compared to active contour methods for segmenting left ventricle. As a quantitative comparison, Computational cost reduced in our proposed method, for example 1.3 times faster than well-known active contour

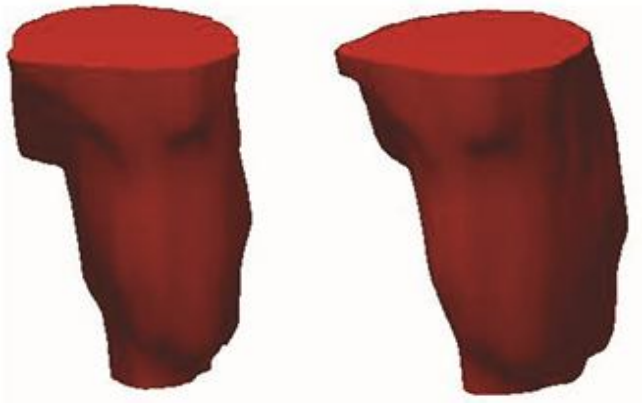

Figure 7. 3-D visualization of left ventricle

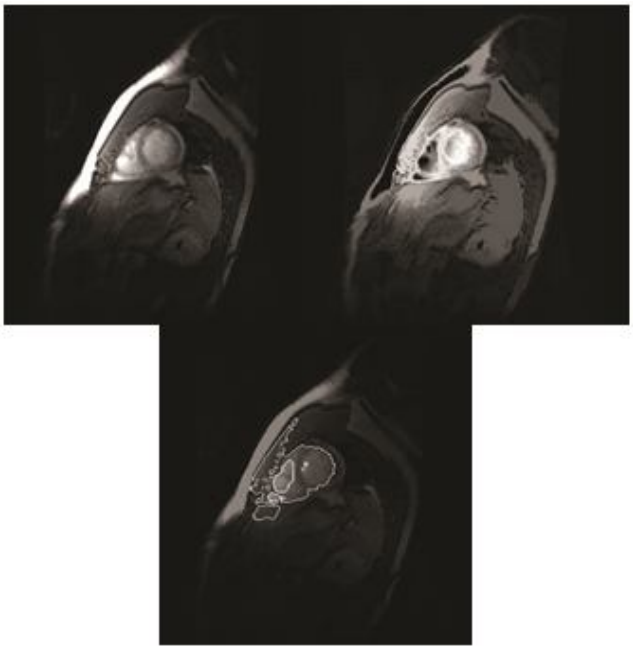

Figure 8. Region growing algorithm defect. In case of not-well-defined LV border, user interaction for providing partial data is undeniable

DOI: 01.IJSIP.4.2.1219

method Chan-Vese [34].One of the limitations which should be mentioned is the influence of the papillary muscle, a muscle surrounding parts of the left ventricle. The problem is that the muscle doesn't fit into the approximated superellipsoidal ventricle shape and, although it should be incorporated into the ventricle volume, it can't easily be separated from the ventricle muscle (myocardium) because both consist of the same tissue type and therefore both have a similar grey-value on a reconstructed image. In addition radiologists do not agree whether the papillary muscle should be included in the ventricle or not.

In this work the papillary muscle will be assumed to be a part of the left ventricle and the impact of this assumption on the different volume estimation techniques will be investigated.

End-diastolic and end-systolic contours in the images were drawn by means of the implemented segmentation tool application. Results of the parametric estimation method are also required for the evaluation, therefore the end-diastolic and end-systolic volume estimation from the patient's diagnosis (performed by an operator after the MR scanning procedure) were provided. To show that different medical operators (and even the same operator at different points of time) tend to produce slightly varying estimation results, the parametric model was applied a second time on each data set by a radiologist. The differing results are of course unintended but nevertheless nearly unavoidable. Different levels of concentration depending on the number of already processed data sets or the tiredness of the operator during the work is one possible explanation. Another one is the experience of the operator with radiological and (in our case) cardiological aspects but also differing interpretations of certain medical aspects can lead to varying results. "Fig. 9," illustrates the correlation of these two estimations.

Table I shows all of the provided information of the image data sets. Columns"EDV1" and"ESV1" contain the results of the parametric volume estimation while columns"EDV2" and"ESV2" contain the older results of the parametric model from the actual patient examination.

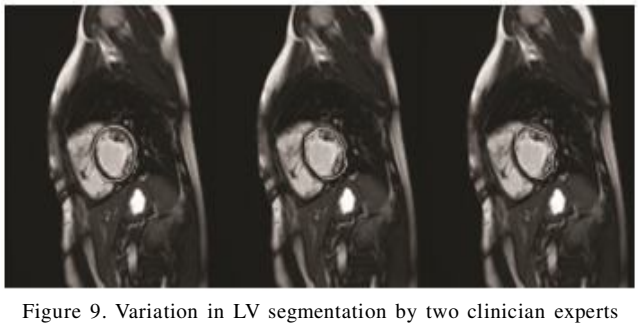

Figure 9. Variation in LV segmentation by two clinician experts

We used four measures to evaluate the segmentation results which are:

- Similarity index: $S_i = \frac{2N_{T_p}}{N_M + N_A} * 100\%$

Where N_{T_p} the number of true positive and N_M is the cardinality of M and N_A is the cardinality of A;

- Jaccard index: $J_i = \frac{N_{T_p}}{N_M + N_A + N_{T_p}} * 100\%$
- Ratio of correct detection (Sensitivity):

$$T_p = \frac{N_{T_p}}{N_M} * 100\%$$

- Specifity: S_E=100-F_p: $F_p = \frac{N_{F_p}}{N_A} * 100\%$

Where N_{F_p} is the number of false positive.

Table. II show evaluation of the fitting superellipse on 17 datasets. Results show that this algorithm can robustly fit a superellipse to a MR cardiac image.

TABLE I. PATIENTS DATASETS WITH VOLUME ESTIMATION RESULTS FROM SUPERELLIPSE MODEL FITTING

P.Num	EDV1[ml]	ESV1[ml]	EDV2[ml]	ESV2[ml]
1	105.9	37.7	106.0	37.9
2	173.2	62.4	182.0	67.3
3	153.8	58.5	153.0	56.6
4	97.1	62.0	97.1	58.1
5	172.1	71.3	173.4	66.6
6	198.0	111.8	202.3	116.2
7	146.3	101.1	145.3	97.5
8	125.0	43.6	125.0	43.8
9	286.6	173.3	288.0	173.3
10	123.4	56.6	123.0	51.2
11	83.2	20.2	81.3	20.0
12	95.4	28	95.2	32.2
13	113.7	22.0	114.6	22.1
14	105.5	18.0	106.5	18.2
15	98.1	19.3	99.1	20.5
16	81.3	27	82.1	29
17	77.4	18.9	75.2	16.8

TABLE II. EVALUATION OF THE FITTING RESULTS OF IMAGES FOR WHICH A MANUAL FITTING WAS AVAILABLE

	Volume metric (%)			
	SI	JI	SE	SP
Average result	80.91	73.28	81.44	90.93

VI. CONCLUTION

In this work we proposed a semi-automatic method that robustly segments and fits superellipse on the left ventricle in cardiac cine MRI images. Superellipse can model a large variety of natural shapes, including ellipse, rectangles, parallelograms, and pinched diamonds, by changing a small number of parameters. Several approaches have been suggested to determine the parameters of superellipses. We used an iterative Levenberg-Marquardt algorithm for this approach that needs partial data to fit superellipse on them. There are several methods that can provide partial data for fitting procedure and a semi-automatic region growing method is used for this approach in this work. This method can significantly reduce the left ventricle segmentation time that is applying manually by radiologists and this is an important point because manually segmentation is a long and tedious

DOI: 01.IJSIP.4.2.1219

task, prone to intra- and inter-expert variability, requires about 20 min per ventricle by an expert clinician.. In this work the papillary muscle will be assumed to be a part of the left ventricle and the impact of this assumption on the different volume estimation techniques will be investigated. We found that using this method is less time consuming than active contour models and because of ellipsoid shape of left ventricle, fitting superellipse on cardiac cine MRI images has maximum accuracy. Further researches can work on calculation of left ventricle functions like Ejection Fraction or stroke Volume from these types of images. They can also develop the automatic methods for providing data points like ellipse fitting methods.

References

[1] AF. Frangi, WJ. Niessen, MA. Viergever, "Three-dimensional modeling for functional analysis of cardiac images: a review," IEEE Trans Med Imaging 20, (2001)

[2] A. Goshtasby, D. Turner, "Segmentation of cardiac cine MR images for extraction of right and left ventricular chambers," IEEE Trans Med Imaging 14(1):56–64

[3] A. Pednekar, U. Kurkure, R. Muthupillai, S. Flamm, "Automated left ventricular segmentation in cardiac MRI," IEEE Trans Biomed Eng 53(7):1425–1428

[4] U. Kurkure, A. Pednekar, R. Muthupillai, S. Flamm, and IA. Kakadiaris, "Localization and segmentation of left ventricle in cardiac cine-MR images," IEEE Trans Biomed Eng 56(5):1360–1370

[5] R. El Berbari, et. al, "An automated myocardial segmentation in cardiac MRI," Conf Proc IEEE Eng Med Biol Soc, pp 4508–4511

[6] N. Paragios, "A variational approach for the segmentation of the left ventricle in cardiac image analysis," Int J Comput Vis 50(3):345–362

[7] A. Chakraborty, L. Staib, and JS. Duncan, "Deformable boundary finding in medical images by integrating gradient and region information," IEEE Trans Med Imaging 15:859–870

[8] A. Singh, D. Goldgof, and D. Terzopoulos, "Deformable Models in Medical Image Analysis," IEEE Computer Society Press, Los Alamitos, CA, USA, 1998.

[9] Y. Zhu, X. Papademetris, AJ. Sinusas, and JS. Duncan "Segmentation of the left ventricle from cardiac MR images using a subjectspecific dynamical model," IEEE Trans Med Imaging 29(3):669– 687

[10] J. Montagnat, and H. Delingette, "4D deformable models with temporal constraints: application to 4D cardiac image segmentation," Med Image Anal 9(1):87–100

[11] T. Cootes, D. Taylor, and J. Graham, "Active shape models – their training and application," Comput. Vis. Image Understand. 61 (1), 38–59.

[12] T. Cootes, G. Edwards, and C. Taylor, "Interpreting face images using active appearance models," Proceedings European Conference on Computer Vision, vol. 2. pp. 484–498.

[13] S. Mitchell, B. Lelieveldt, R. Van Der Geest, J. Bosch, J. Reiber, and M. Sonka, "Multistage hybrid active appearance model matching: segmentation of left and right ventricles in cardiac MR images," IEEE Trans. Med. Imag. 20 (5), 415–423.

[14] M. Dulce, G. Mostbeck, K. Friese, G. Caputo, and C. Higgins, "Quantification of Left Ventricular Volumes and Function with Cine MR Imaging: Comparison of Geometric Models with Three- Dimensional Data," Radiology **188** (1993), pp. 371–376.

[15] A. Goshtasby and D. A. Turner, "Segmentation of Cardiac Cine MR Images for Extraction of Right and Left Ventricular Chambers," IEEE Transactions on Medical Image Processing **14** (1995), no. 1, pp. 56–64.

[16] J. Weng, A. Singh, and M.Y. Chiu, "Learning-Based Ventricle Detection from Cardiac MR and CT Images," IEEE Transactions on Medical Image Processing 16 (1997), no. 4, pp. 378–391.

[17] D. Geiger, A. Gupta, L. Costa, and J. Vlontzos, "Dynamic programming for detecting, tracking and matching deformable contours," IEEE Trans. Pattern Anal. Machine Intell. 19 (6), 294–302.

[18] N. Paragios, "A variational approach for the segmentation of the left ventricle in cardiac image analysis," Int. J. Comput. Vis. 50 (3), 345–362.

[19] I. Ben Ayed, S. Li, and I. Ross, "Embedding overlap priors in variational left ventricle tracking," IEEE Trans. Med. Imag. 28 (12), 1902–1913.

[20] C. Petitjean, and J.N. Dacher, "A review of segmentation methods in short axis cardiac MR images," Medical Image Analysis 15, 169–184 (2011).

[21] P. Pentland, "Perceptual organization and the representation of natural form," *Artif. Intell.*, vol. 28, pp. 293–331, 1986

[22] M. Gardiner, "The superellipse: a curve that lies between the ellipse and the rectangle," *Sci. .4m.,* 1965, 21, pp. 222-234

[23] A.H. BARR, "Superquadrics and angle-preserving transformations," *IEEE Comput. Graph. Appl.,* 1981, 1, pp. 11-23

[24] A. Pentland, "Perceptual organisation and the representation of natural form," *Art$ Intell.,* 1986, 28, pp. 293-331

[25] Z. ZHANG, "Parameter estimation techniques: a tutorial with application to conic fitting," *Image* Vis. *Comput.,* 1997, 15, pp. 59-76

[26] X. Zhanga, and P. L. Rosin, (2003) "Superellipse fitting to partial data," Pattern Recognition, Vol 36(3), 743-752

[27] M. Ghelich Oghli, A. Fallahi, V. Dehlaqi, M. Pooyan, and N. Abdollahi, "A Novel Method for Left Ventricle Volume Measurement on Short Axis MRI Images Based on Deformable Superellipses," SPIT 2012, LNICST pp. 102–107, 2012.

[28] S.A. Hojjatoleslami, and J. Kittler, "Region growing: a new approach," IEEE Transactions of Image Processing, vol.7, no.7, July 1998, pp.1079-84

[29] M. Ghelich Oghli, A. Fallahi, and M. Pooyan, "Automatic Region Growing Method using GSmap and Spatial Information on Ultrasound Images," In: 18th Iranian Conference on Electrical Engineering, May 11-13, pp. 35-38 (2010)

[30] K. Levenberg (1944), "A Method for the Solution of Certain Non-Linear Problems in Least Squares," The Quarterly of Applied Mathematics 2: 164–168. A. Girard (1958). Rev. Opt 37: 225, 397

[31] P. L. Rosin, "Fitting superellipses," IEEE Trans. Pattern Anal. Machine Intell., vol. 22, pp. 726–732, July 2000

[32] M. Mancas, B. Gosselin and B. Macq, "Segmentation Using a Region Growing Thresholding," 4th Image processing : algorithms and systems ,2005, v.56, pp. 388-398

[33] P. Rosin, and G. West, "Curve segmentation and representation by superellipses," Proc. IEE: Vision Image Signal Process. 142 (1995) 280–288

[34] T.F. Chan, and L.A. Vese, "Active contours without edges," IEEE Transactions on Image Processing, 10(2):266–277.

DOI: 01.IJSIP.4.2.1219